سن سنجی، ژئوشیمی رادیو ایزوتوپ‌ها و منشا مونزوگرانیت پالئوتتیس سنگ بست مشهد، ایران

محمد حسن کریم‌پور*۱، لنگ فارمر۲، چاک استرن۲

۱- مرکز پژوهشی اکتشاف ذخایر معدنی شرق ایران، دانشگاه فردوسی مشهد

۲- گروه زمین شناسی دانشگاه کلرادو، بولدر امریکا

چکیده: منطقه مطالعه در شمال شرق ایران و در جنوب مشهد واقع شده است. اقیانوس پالئوتتیس در اردویسین شروع به باز شدن نمود و فرورانش صفحه اقیانوسی به زیر صفحه توران از اواخر دونین آغاز گردید. راندگی صفحه توران روی صفحه ایران در آواخر کارنین (۲۲۵Ma) شروع شد و در این مقطع زمانی هیچگونه صفحه اقیانوس پالئوتتیس باقی نمانده بود. دو مرحله دگرگونی ناحیه شناسایی شدند: اولین با گوهزایی هرسینین (اواخر پالئوزوئیک) و دومین با گوهزایی سیمرین (ژوراسیک) مرتبط است. مونزوگرانیت در بقایای پوسته اقیانوس پالئوتتیس نفوذ نموده است (متاافیولیت و متافلیش). مونزوگرانیت به لحاظ شیمیایی گرانیت نوع S و فوق آلومینیوم متوسط است. عدد پذیرفتاری مغناطیسی مونزوگرانیت پایین است [SI 10^{-5} × (5 to 11)] و لذا مربوط به سری ایلمینیت هستند. مونزوگرانیت دارای غنی شدگی عناصر کمیاب سبک و کاهیدگی عناصر کمیاب سنگین هستند. تمامی نمونه‌ها دارای بی‌هنجاری منفی Eu هستند (Eu/Eu* = 0.62 to 0.88). میزان کل عناصر کمیاب بین ۴۸۱-۲۱۲ ppm است. سن سنجی مونزوگرانیت به روش U-Pb در کانی زیرکون انجام و سن 201.3 ± 3.6 Ma تعیین شد (راتین، تریاس فوقانی). نسبت ایزوتوپ اولیه ($^{87}Sr/^{86}Sr$)i و ($^{143}Nd/^{144}Nd$)i در مونزوگرانیت به ترتیب 0.706776 و 0.512219 اندازه‌گیری و محاسبه شد (با توجه به سن ۲۰۱ میلیون سال). نسبت ایزوتوپ اولیه ($^{87}Sr/^{86}Sr$)i و ($^{143}Nd/^{144}Nd$)i اسلیت به ترتیب 0.72061 و 0.511601 محاسبه شد (با توجه به سن ۲۰۱ میلیون سال). ایزوتوپ اولیه εNd در مونزوگرانیت 3.13- و در اسلیت -15.19 اندازه گیری شد. براساس داده‌های ایزوتوپی و عناصر کمیاب ماگمای اولیه مونزوگرانیت از بخش تحتانی پوسته قاره‌ای یا از جبه منشا گرفته و در پوسته قاره‌ای ضمن بالا آمدن آلودگی صورت پذیرفته است.

واژه‌های کلیدی: مشهد، پالئوتتیس، مونزوگرانیت، *Rb-Sr, Sm-Nd, U-Pb*

* نویسنده مسئول، تلفن: ۸۷۹۷۲۷۵ (۰۵۱۱) ۹۸+، نمابر: ۸۷۹۷۲۷۵ (۰۵۱۱) ۹۸+، پست الکترونیکی: mhkarimpour@yahoo.com

Geochronology, Radiogenic Isotope Geochemistry, and Petrogenesis of Sangbast Paleo-Tethys Monzogranite, Mashhad, Iran

M. H. Karimpour[1*], G. L. Farmer[2], C. R. Stern[2]

1. Research Center for Ore Deposits of Eastern Iran, Ferdowsi University of Mashhad P.O. Box No. 91775-1436, Mashhad, Iran
2. Dept. of Geological Sciences, University of Colorado, CB-399, Boulder, CO, USA

Abstract: The study area is located in northeastern Iran (south of Mashhad). Paleo-Tethys Ocean opened during Silurian time and subduction under Turan plate was started in Late Devonian. By Late Triassic (225 Ma) there was no Paleo-Tethys left on an Iranian transect, therefore Turan plate obducted over Iran Plate. Two stages of low grade regional metamorphism are exposed, that are related to Hercynian (Late Paleozoic) and Cimmerian (Jurassic) orogenies. The Paleo-Tethys remnants (meta-ophiolite and meta-flysch) were intruded by Sangbast monzogranite. Chemically, monzogranite is moderately peraluminous S-type granitoid. It has low values of magnetic susceptibility [(5 to 11) $\times 10^{-5}$ SI] therefore it is classified as belonging to the ilmenite-series of reduced type granitoids. Monzogranite is characterized by strong light rare earth element (LREE) enrichment and less low heavy REE (HREE). All samples have very small negative Eu anomalies (Eu/Eu* = 0.62 to 0.88). Total REE content of monzogranite is between 212-481 ppm. The result of U-Pb zircon age dating of monzogranite is 201.3 ± 3.6 Ma (Upper Triassic, Rhaetian time). The initial $^{87}Sr/^{86}Sr$ and $^{143}Nd/^{144}Nd$ ratios for monzogranite is (0.706776 and 0.512219) when recalculated to an age of 201 Ma, consistent with the new radiometric. The initial $^{87}Sr/^{86}Sr$ and $^{143}Nd/^{144}Nd$ ratios for slate is (0.720613 and 0.511601) respectively when recalculated to an age of 201 Ma, consistent with the new radiometric results. Initial εNd isotope values for monzogranite is -3.13 and the slate is -15.19. Based on radiogenic isotopic data and REE monzogranite magma originated either from lower continental crust which was very different from slate or it is originated from mantle and contaminated in continental crust during ascending.

Keywords: *Mashhad, Paleo-Tethys, monzogranite, Rb-Sr, Sm-Nd, U-Pb.*

Introduction

The study area is located in northeastern Iran and lies between Longitude 59° 15′ E to 59° 45′ E and Latitude 36° N to 36° 30′ (Fig. 1). The Binaloud Mountains are part of Paleo-Tethys remnants meta-ophiolites and meta-flysch) which are intruded by tonalite, granodiorite, monzogranite, biotite-muscovite leucogranite and pegmatite dikes at different episodes (Triassic to Cretaceous).

The Binaloud Mountains are situated south and west of Mashhad city. The southern and western part of Mashhad city is built on the remnant of the Paleo-Tethys and the younger intrusive rocks (Fig.1).

---

[*]Corresponding author, Tel.: +98 (0511) 8797275, Fax: +98 (0511) 8797275, Email: mhkarimpour@yahoo.com

Jarchovski et al., [1] carried out some mineral reconnaissance on monzogranite, granite, tonalite, ophiolite and metamorphosed rocks within Binaloud region. The earliest petrography study on Mashhad granites is carried by Albertie & Moazez [2]. K-Ar ages of muscovite and biotite (4 samples) from two localities within the main granite body gave the following ages: 145, 120, 135 and 146 (± 3) Ma (Late Jurassic Early Cretaceous) [3]. Pebbles and cobbles of tonalite, granodiorite and monzogranite are found within the conglomerate of Early Jurassic. This indicates that the intrusive rocks were intruded at different time. Plimer & Moazez [4] had studied the petrography of Dehnow tonalite and the xenocryst garnets. Majidi [5] did a Ph.D thesis on the,

ophiolite, metamorphic rocks and the granite rocks. Alavi [6-8] had studied the structural characteristics of the area in detail. Valizadeh & Karimpour, [9] studied petrography and major elemental of the granitoids. Mirnejad [10] did M.Sc. thesis on the petrography and major elements content of intrusive rocks. Iranmanesh & Sethna [11] did a general study on Mashhad granites. Abbasi [12] studied metamorphic rocks of part of the study area both on regional and contact metamorphism. Ghazi et al., [13] studied the geochemistry and determined age of the Mashhad Ophiolite.

All of these studies, so far, did not study the age, petrogenesis, and tectonic setting of monzogranite.
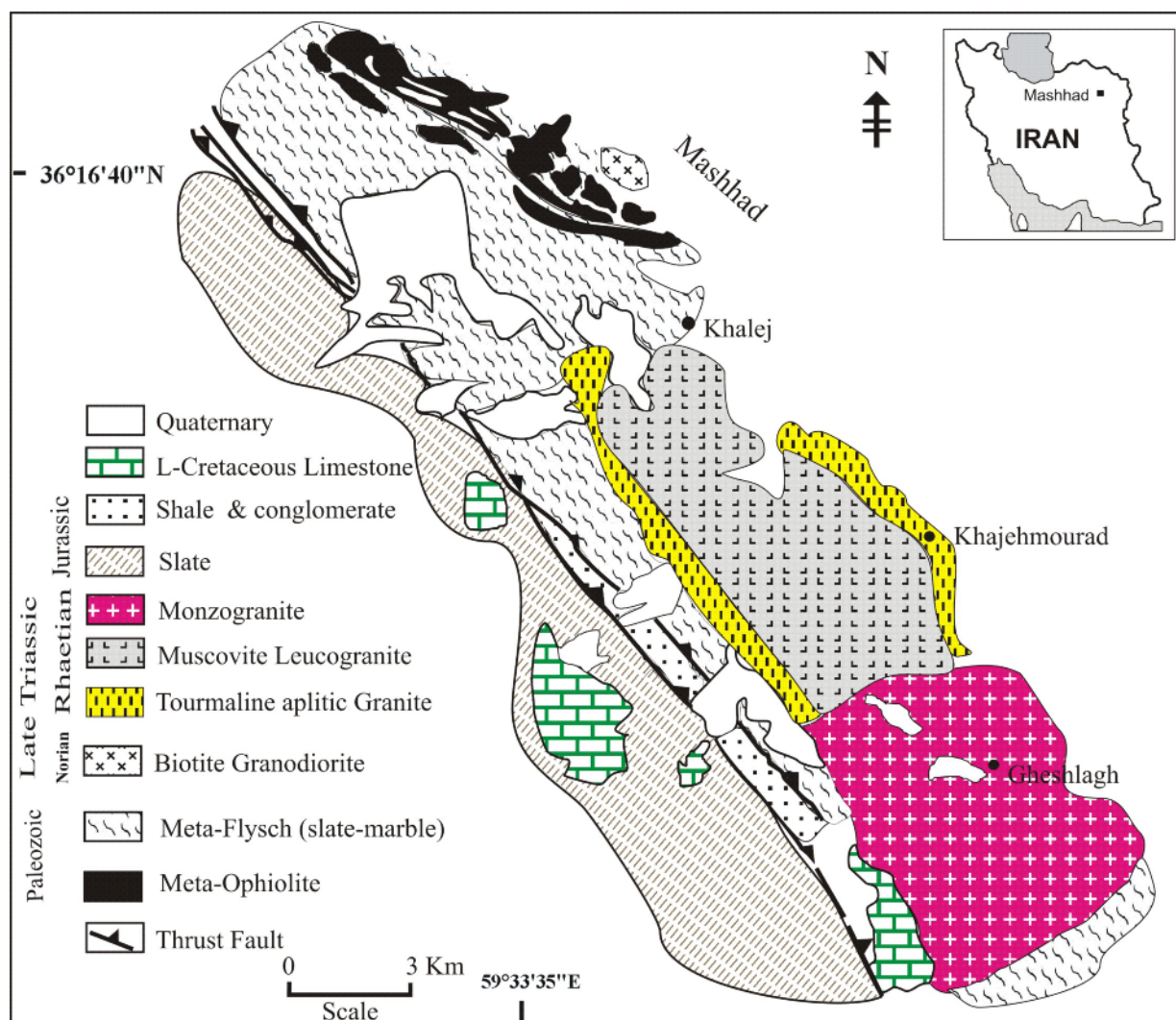

Figure 1 Geological map showing monzogranite and other rock unites.

Geogical setting

During the Paleozoic Iran and Turan plates formed a coherent unit and were separated from the Turan Plate by the Paleo-Tethys Ocean. Based on the work and research by Stampfli, [14-18], there are very good evidence in the Alborz and elsewhere that the Paleo-Tethys opened in Silurian time. In the Late Paleozoic or in Early Triassic, the Iran Plate drifted away from Arabia plate by the opening of the Neo-Tethys Ocean and Iranian microcontinent collided with the Turan Plate. In Iran, Turkey and Greece the closure of Paleo-Tethys did not took place before the Late Triassic (231 Ma). By the Late Triassic (about 225 Ma) it is quite certain that there was no Paleo-Tethys left on an Iranian transects [14, 16 - 19].

The Binaloud region in northeastern Iran, south of Mashhad, is the remnant of Paleo-Tethys (Fig. 1). To the west, it extends to Alborz Mountains and then to Azerbaijan, Armenia, Turkey and other parts of Europe. Toward the east, it extends to Hindu-Kush Mountains north of Afghanistan and India. The obduction of the Paleo-Tethys remnants and their emplacement over the Iranian micro continental margin must have been per-Late Triassic [14, 16-19]. It is concluded by Alavi [8] and Stockline [19], that the initiation of the Iranian microcontinent-Turan collisional processes had also been started prior to the end of Triassic.

The obducted remnants of the Paleo-Tethys Ocean in Binaloud area, Iran, is composed of several rock assemblages including: meta-ophiolite, meta-flysch and some submarine pyroclastics. Two episodes of regional metamorphisms are recognized in the study area. The first stage took place during initial stage of collision. It may be related to Hercynian orogeny which occurred during the Late Paleozoic time. Only rocks are effected by the green schist facies are exposed. Slates are dominated with minor phyllite. The second regional metamorphism occurred sometimes in Jurassic time. This is corresponded to Cimmerian orogeny (Jurassic).

Ophiolites are exposed mainly along the northern part of the belt (Fig. 1). They can be divided into two complexes: 1) Nourabad and 2) Chehar-Cheshmeh. The Nourabad complex (Virani is the older name) is exposed along the road from Mashhad to Shandiz (about 25 km from Mashhad) around the village of Nourabad (Fig. 1). The Chehar-Cheshmeh ophiolite complex is exposed between Vakilabad and Khlaj (Fig. 1). The southwestern city of Mashhad is mainly built on this complex. Hornblende gabbros was dated by ^{40}Ar-^{39}Ar (281.4 Ma and 277.4 Ma) corresponding to isochrone ages of 287.6 and 281.7 Ma. In a separate K/Ar analysis, the same two samples gave values of 273 and 265 Ma, suggesting Late Pennsylvanian-Early Permian ages, same, Paleo-Tethys age for the oceanic crust [13].

Slates, quartzite, marble, minor phyllite, carbonate conglomerate and olistostromes are considered as deep water flysch sediments deposits Alavi [6]. No fossil was found within this unit.

The second low grade meta-sediments, consist of thick sequence of low grade metamorphosed shale and siltstones with basal conglomerate. Conglomerate contains pebbles of ophiolite, Meta-flysch, tonalite and granodiorite. Conglomerate is cut by the thrust fault in the northern part (Fig. 1). Due to thrusting, the basal conglomerate is highly sheared and silicified. Within the thrust zone there is a highly brecciated dolomite (Fig. 1). The shale contains plant fossils which are dated Early Jurassic [20]. The second regional metamorphism must be occurred sometimes after Early Jurassic. Within a narrow NW-SE tectonic basin, Jurassic conglomerate, shale and siltstone are being deposited (Fig. 1). The basal conglomerate is formed in the northern part of the basin and changed to siltstone and shale in a SW direction. The basal conglomerate contains pebbles and cobbles from meta-flysch, tonalite, granodiorite, monzogranite and leucogranite. There is small coal bearing horizons within the shale. Plant fossils are abundant. Based on the plants fossils, the age of this sequence is Lias-Dogger [20].

Early Cretaceous rocks are exposed in the southern part of the study area (Fig.1). There are two rock types: a lower conglomerate and an upper limestone.

Analytical methods
Bulk-rock chemistry
Intrusive rocks were selected and they were analyzed for major, trace and rare earth elements. Major elements were analyzed by wavelength-dispersion X-ray fluorescence spectrometry (XRF) using fused discs. Pressed powder pellets were used for Zr, Nb, Sn, Sr, Ba, Sc, Y and Ga measurements by XRF (The XRF spectrometer used in this study was a Philip PW 1410) at Ferdowsi University of Mashhad, Iran. REE

composition of rocks was determined by ICP-MS in Canada (Acme Lab. Canada). FeO and Fe_2O_3 content were determined by titration with standardized potassium permanganate solution with precision of ±1 % at Ferdowsi University of Mashhad, Iran.

U/Pb dating

Two rock samples, which were both analyzed for Sr and Nd isotopes, were chosen for zircon U-Pb age dating. Zircons were isolated using standard mineral separation techniques. From each rock about 70 zircon grains were separated. Zircons were mounted along with a zircon standard and a couple of chips of NBS 610 Trace Element Glass) in epoxy and polished down to 20 μm. Zircon age dating was done at the Arizona LaserChron Center with the method of Gehrels, G. E., and V. Valencia, [21]. Cathode-luminescence (CL) images are acquired for samples to be analyzed because they provide a powerful tool for placing laser pits in homogeneous portions of crystals, and also can help determine the origin (e.g., igneous, metamorphic, hydrothermal) of zircon grains. Laser ablation takes place with a beam diameter of either 35 or 25 microns for most applications, or with a beam diameter of 15 or 10 microns if finer spatial resolution is needed. With a 35 or 25 micron beam, the laser is set at a repetition rate of 8 Hz and energy of 100 mJ, which excavates at a rate of ~1 micron per second. This generates a signal of ~100,000 cps per ppm for U in zircon. For smaller beam sizes, the ablation rate is reduced to ~0.5 micron/second by reducing the laser energy (60 mJ) and repetition rate (4 Hz). In both cases the ablated material is removed from the ablation chamber in He carrier gas. The carrier gas (and sample) is then mixed with Ar gas before entering the plasma of the Inductively Coupled Plasma Mass Spectrometer (ICPMS). Isotopic analysis is performed with a Multicollector Inductively Coupled Plasma Mass Spectrometer (GVI Isoprobe) that is equipped with an S-option interface. The instrument is equipped with a collision cell that is operated with a flow rate of 0.2 ml/min of argon to create a uniform energy distribution, and the accelerating voltage is ~6 kV. Collectors include nine Faraday detectors and four low-side channeltron multipliers, all of which are moveable, as well as an axial Daly photomultiplier.

Nd–Sr isotopes Sr and Nd isotopic analyses were performed on a 6-collector Finnigan MAT 261 Thermal Ionization Mass Spectrometer at the University of Colorado, Boulder (USA). $^{87}Sr/^{86}Sr$ ratios were analyzed using four-collector static mode measurements. Thirty measurements of SRM-987 during study period yielded mean $^{87}Sr/^{86}Sr = 0.71032 ± 2$ (error is the 2 sigma mean). Measured $^{87}Sr/^{86}Sr$ were corrected to SRM-987 = 0.71028. Error in the 2 sigmas of mean and refer to last two digits of the $^{87}Sr/^{86}Sr$ ratio. Measured $^{143}Nd/^{144}Nd$ normalized to $^{146}Nd/^{144}Nd=0.7219$. Analyses were dynamic mode, three-collector measurements. Thirty-three measurements of the La Jolla Nd standard during the study period yielded a mean $^{143}Nd/^{144}Nd = 0.511838 ± 8$ (error is the 2 sigma mean).

Petrography

Monzogranite is exposed in the southeastern plutonic belt of Mashhad (Fig. 1). It contains 32 to 40 %, quartz, 32 to 42 %, K-feldspar, 8 to 17 %, plagioclase, 5 to 10 %, biotite and minor muscovite. Accessories phases are zircon and apatite. Monzogranite has a coarse grained texture with typically coarse pink K-feldspar phenocrysts (2-3 cm long). Weak to moderate foliation fabric occurs in some parts within monzogranite which is formed by alignment of feldspars. This fabric seems to have formed by magmatic to possibly sub-magmatic processes with a weak solid-state overprint.

Geochemistry

Major and trace elements

The results of elemental analyses from monzogranite are presented in Table 1. Ternary plot of Ab-Or-An [22] shows that monzogranite plotting within the boundary of granite and quartz monzonite; therefore they are named as monzogranite (Fig. 2). Monzogranite name was given to this intrusive based on this Diagram.

A discrimination plot of 1000Ga/Al versus Y [23] shows that monzogranite plots within the field of I- and S-type granitoids (Fig. 3).

Barbarin [24] classified granitoid rocks based on their origin and their geodynamic environments. Based on his classification, monzogranite is belonging to K-rich calc-alkaline granitoids (KCG) type (Fig. 4).

Table 1. Major and trace elements analysis of monzogranite

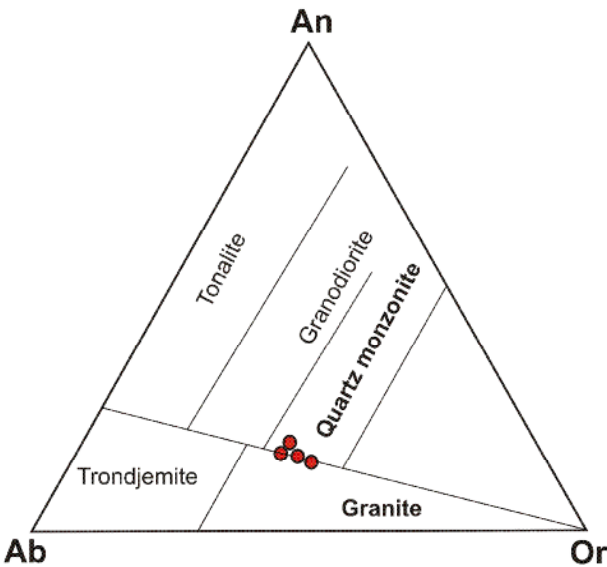| Oxides%	FG-1	FG-4	FG-5	G-15	G-14	G-13	Fi-1	Fi-2	Fi-3
SiO_2	67.48	68.59	67.2	63.94	65.82	67.25	64.55	63.63	66.70
TiO_2	0.45	0.39	0.41	0.48	0.40	0.39	0.59	0.45	0.38
Al_2O_3	15.76	15.65	15.5	15.91	15.85	15.01	14.81	15.37	14.26
Fe_2O_3	0.81	0.73	0.75	3.9	2.4	2.2	3.98	3.65	2.85
FeO	2.25	2.07	2.15	1.2	0.95	0.85	1.25	1.2	1.1
MnO	0.10	0.08	0.09	0.14	0.16	0.13	0.15	0.17	0.11
MgO	1.08	1.0	1.1	1.40	1.07	1.08	1.77	1.14	1.00
CaO	2.13	2.19	2.14	2.45	2.17	1.96	2.75	3.06	2.07
Na_2O	3.49	3.57	3.45	3.90	4.05	3.70	3.45	3.91	3.50
K_2O	4.58	4.17	4.52	4.81	4.80	5.40	5.49	5.50	5.84
P_2O_5	0.10	0.25	0.15	0.26	0.30	0.22	0.31	0.29	0.22
H_2O (+)	1.04	0.91	1.1	1	1.2	1.25	0.85	1.1	1.2
Total	99.41	99.73	99.78	99.39	99.17	99.44	99.95	99.47	99.23
Norm (CIPW)									
Q	25.31	25.42	22.79	13.7	17	18.5	14	11.1	17.5
C	1.43	1.84	1.4	0.45	0.5	0.05	0	0	0
Or	27.26	24.97	26.68	28.4	28.3	31.9	32.4	32.5	34.6
Ab	29.74	30.61	29.16	33	34.3	31.3	29.2	33.1	29.7
An	9.91	9.52	9.68	10.4	8.8	8.3	8.7	8.2	5.6
Hy	5.67	5.26	5.55	9.125	5.92	5.6	8.7	5.9	5.1
Mt	1.18	1.07	1.09	1.7	1.4	1.2	1.8	1.7	1.6
Il	0.82	0.75	0.78	0.9	0.7	0.74	1.1	0.85	0.72
Ap	0.24	0.6	0.33	0.61	0.71	0.52	0.73	0.7	0.5
Trace (ppm)									
Sn	5.1	6	-		7	4	5	6	6
Rb	180.8	181.5	181.2	279	236	244	178	169	236
Sr	584.2	535	543	1011	744	832	732	1139	573
Ba	1093	886	968	1671	976	1320	1310	1534	808
Nb	40.9	50.1	46.2	68	73	57	38	76	47
Zr	188	182	187	255.5	243.9	202.1	233.4	305.3	173.8
Ga	20	18	17.8	-	-	-	-	-	-
Sc	5.12	4.78	-	-	-	-	-	-	-
Rb/Sr	0.3	0.33	0.32	0.27	0.31	0.29	0.24	0.14	0.41
Rb/Ba	0.16	0.204	0.18	0.16	0.24	0.18	0.13	0.11	0.29

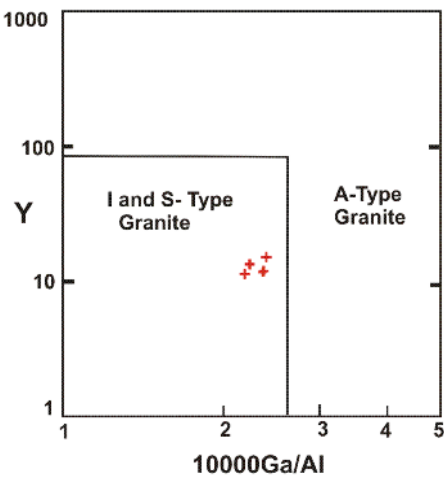**Figure 2.** Triangle An-An-Or shows that monzogranite plot within the boundary of granite and quartz monzonite [22].

Figure 3. Plot of Y versus 1000Ga/Al show that monzogranite plot in the field of I-S type granite [23].

Figure 4. Monzogranite plot in the field of KCG (K-rich calc-alkaline granitoids [24].

Multi-cationic plot of Villaseca [25] shows that monzogranite plot in the field of moderately peraluminous granitoids (M-P) (Fig. 5) Since they are above the I-S line (Fig. 5) therefore they are S-type granitoid.

Trace and rare earth elements (REE)
Plot of R1 versus R2 show that monzogranite plot in the field of syn and late collision (Fig. 6) [26]. The low field strength elements (LFSE) (Rb, Ba and Sr) content of monzogranite are in general

high (Table 1). The Rb/Sr is between 0.14 and 0.41 in monzogranite (Table 1). The Ba content of monzogranite is between 808-1534 ppm which is very high. This indicates that the K-feldspar content of the source rock was high and they are completely melted.

REE analyses of selected samples from the monzogranite are shown in Table 2. Chondrite-normalized REE patterns (Fig. 7), of monzogranite characterized by strong light rare earth element (LREE) enrichment and less low heavy REE (HREE) content. All samples have very small negative Eu anomalies (Eu/Eu* = 0.62 to 0.88). According to Taylor and McLennan [27], the term Eu/Eu* is calculated by: Ratios of Eu/Eu* > 1.0

indicate positive, Eu/Eu* < 1.0 negative anomalies. Total REE content of monzogranite is between 212-481 ppm (Table 2).

Rock/orogenic normalized spidergrams of representative sample from monzogranite are plotted in Fig. 8. Well defined negative anomalies are observed for Ta, Hf, Y and Yb. Rb, Th, Nb, Sm and Ce show positive anomalies (Fig. 8). Rb shows the highest positive anomaly (Fig. 8). High Rb indicates that the magma originated from a source with high feldspar and most of the feldspar was melted. Monzogranite contain high K_2O, with high potassium feldspar. Th content of this rock is very high (Fig. 8).
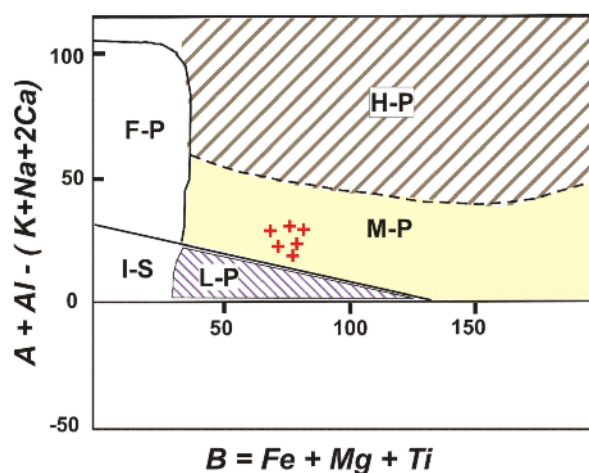

Figure 5. Monzogranite plotted in the field of moderately per-aluminous granitoids (M-P) [25].
(L-P = low peraluminous; M-P = moderately peraluminous; H-P = highly peraluminous; F-P = felsic peraluminous).
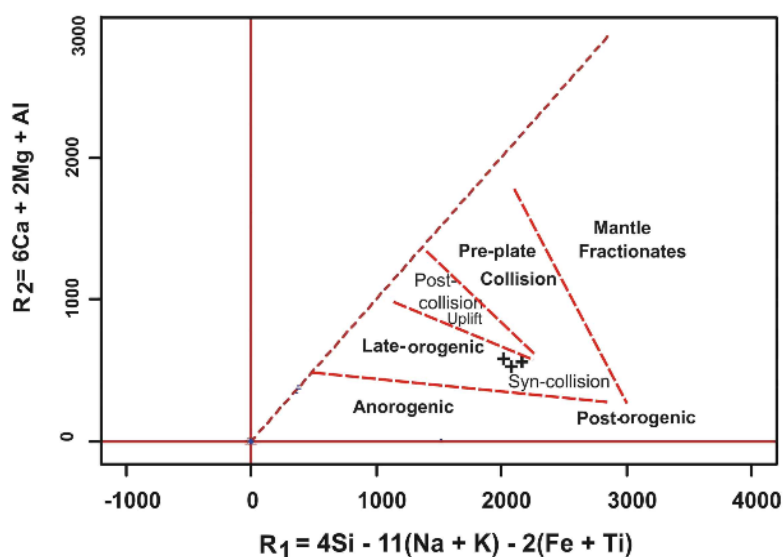

Figure 6. Plot of R1 versus R2 shows that monzogranite plot in the field of syn and late collision [26].
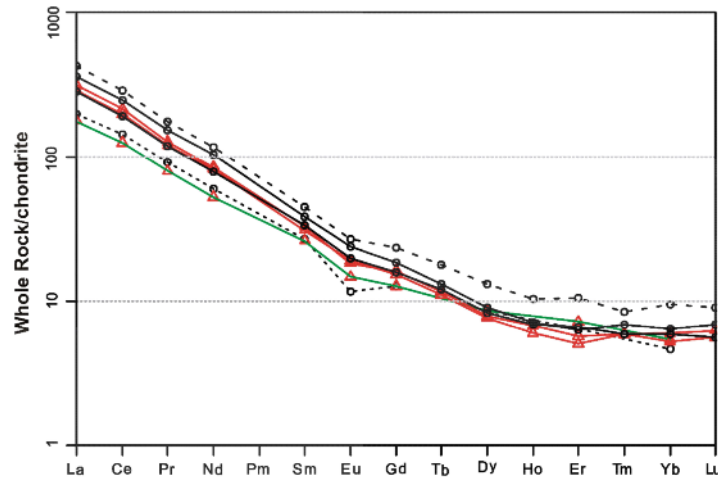
Figure 7. Chondrite-normalized REE distribution of monzogranite (Chondrite-normalized, Boynton [28].

Table 2. Rare earth elemental analysis of monzogranite

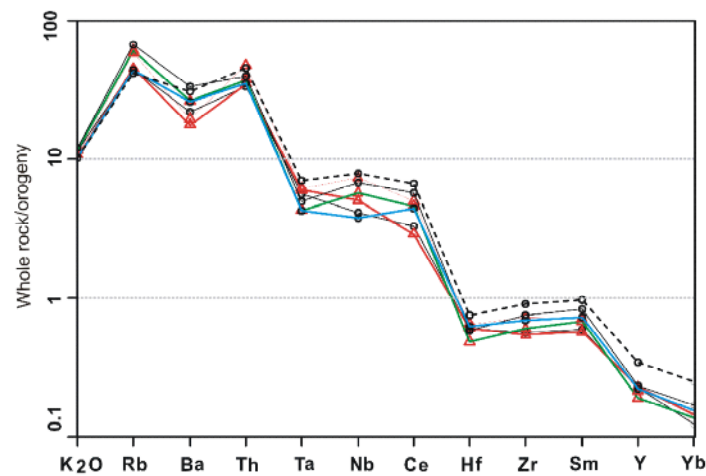| REE (ppm)	FG-1	FG-4	G-13	G-14	G-15	Fi-1	Fi-2	Fi-3
La	61.2	54.93	89.2	97.4	11.8	87.3	132.4	58.6
Ce	115.1	101.15	160.5	174	199.7	153.5	232.9	107.7
Pr	11.15	9.72	14.7	15.5	18.6	14.56	21.45	9.46
Nd	35.86	31.46	49.2	50.9	62	47.3	69.9	31.6
Sm	5.27	5.09	6.05	6.38	7.49	6.49	8.74	4.31
Eu	0.85	1.08	1.39	1.34	1.74	1.45	1.95	0.98
Gd	3.27	3.29	3.94	4.19	4.78	4.11	6.02	3.06
Dy	2.76	2.73	2.46	2.51	2.88	2.67	4.23	1.89
Er	1.34	1.51	1.05	1.19	1.32	1.38	2.19	0.92
Yb	0.97	1.13	1.08	1.24	1.33	1.22	1.97	0.97
Sum	237.77	212.09	295.3	354.65	311.64	319.98	481.75	219.49
(La/Yb)N	42.537	32.773	55.683	52.957	56.673	48.244	45.311	40.73
Eu/Eu*	0.626	0.807	0.871	0.792	0.889	0.858	0.826	0.825
(La/Sm)N	7.305	6.788	9.274	9.603	9.389	8.461	9.529	8.553
(Eu/Yb)N	2.492	2.718	3.66	3.073	3.72	3.38	2.829	2.873

Figure 8. Rock/orogenic normalized spidergrams of representative sample from monzogranite (Rock/orogenic normalized based on Pearce et al., [29]).

U-Th-Pb Zircon age dating

Majidi [30] dated Dehnow and Kuhsangi granodiorite and diorite using K-Ar method came out with ages of 256 to 245 Ma. The Paleo-Tethys remnants (meta-ophiolite and meta-flysch) were intruded by Sangbast monzogranite. Ghazi et al., [13] determined age of the Mashhad meta-ophiolite (273 and 265 Ma). By Late Triassic (225 Ma) there was no Paleo-Tethys left on an Iranian transect, therefore Turan plate obducted over Iran Plate. Since monzogranite rocks were intruded during the collision of Iranian plate with Turan plate, their age must be younger than 225 Ma. Therefore the K-Ar age (256 to 245 Ma) of Majidi [5] is not correct.

From the monzogranite (sample Fi-1) 70 zircon grains were separated. Cathode-luminescence (CL) images are acquired from zircon to be analyzed because they provide a powerful tool for placing laser pits in the homogeneous portions of crystals (Fig. 9).

The results of U-Th-Pb zircon analysis from monzogranite are presented in the Tables (3). The results of calculation of isotopic age are presented on the Concordia plot diagram (Fig. 10). Based on 23 analyzed points the mean age value (weighted mean) is of 201.3 ± 3.6 Ma (error in the 2 sigmas level). Based on U-Th-Pb zircon age dating, the Mashhad monzogranite was formed in Upper Triassic (Rhaetian) time.

Rb-Sr and Sm-Nd Isotope composition

Sr and Nd isotope data for representative monzogranite and slate samples are given in Table (4 & 5). The initial $^{87}Sr/^{86}Sr$ and $^{143}Nd/^{144}Nd$ ratios for monzogranite is (0.706776 and 0.512219, respectively), when recalculated to an age of 201 Ma, consistent with the new radiometric results (Table 4 & 5). The initial $^{87}Sr/^{86}Sr$ and $^{143}Nd/^{144}Nd$ ratios for slate is (0.702061 and 0.511601, respectively), when recalculated to an age of 201 Ma, consistent with the new radiometric results (Table 4 & 5). Initial εNd isotope values for monzogranite are -3.13 and for the slate is -15.19 (Table 5). The values for the plutonic rocks could be considered as representative of magma derived from lower continental crust or upper mantle which is contaminated by the crust.
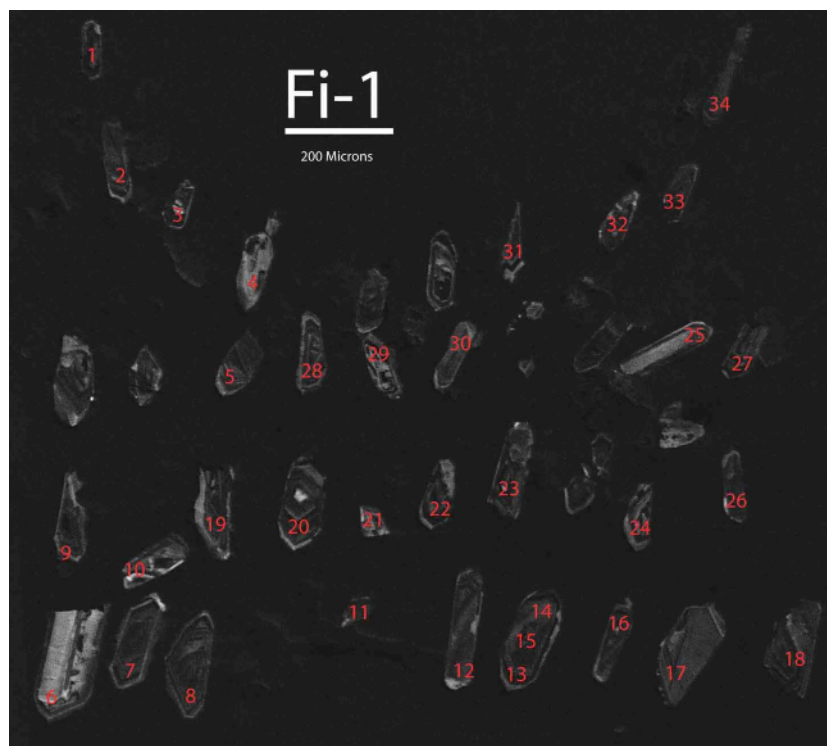

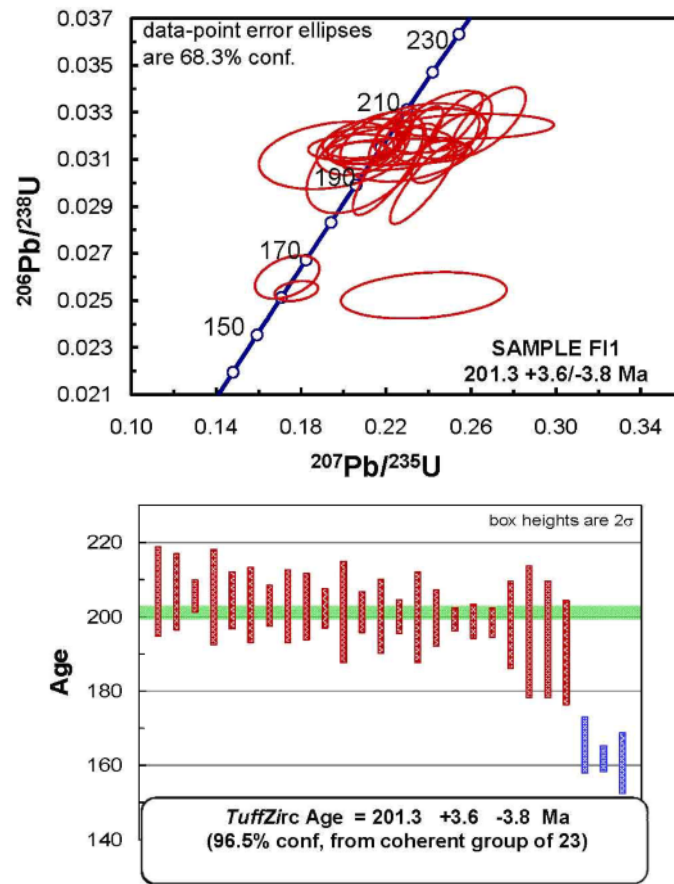**Figure 9** Cathode-luminescence (CL) images of zircon from monzogranite

Figure 10. (a) Concordia plot of $^{207}Pb/^{235}U$ versus $^{206}Pb/^{238}U$ for calculating the age of zircons (monzogranite): (b) TuffZirc graphics calculating the age of zircons (monzogranite) (ellipses are $\pm 2\sigma$).

Table 3. Data of U-Pb-Th Laser-Ablation Multicollector ICP Mass Spectrometry analysis of zircon from monzogranite (Fi-1).

analysis	U (ppm)	$^{206}Pb/^{204}Pb$	U/Th	$^{206}Pb/^{207}Pb$	± (%)	$^{207}Pb/^{235}U$	± (%)	$^{206}Pb/^{238}U$	± (%)	Age (Ma)	± (%)
1	1068	1112	1.4	20.9134	5.9	0.2091	6.0	0.0317	1.4	201.3	2.7
2	1018	946	0.8	20.8012	6.4	0.2091	6.9	0.0315	2.5	200.2	5.0
3	717	586	0.3	20.7634	4.2	0.2077	4.3	0.0313	1.0	198.6	2.0
4	800	2394	3.4	17.3954	2.2	0.2375	4.3	0.0300	3.8	190.3	7.1
5	490	10238	3.8	19.7732	2.2	0.2230	2.6	0.0320	1.4	203.0	2.8
6	1106	5632	5.6	18.7072	2.1	0.2350	2.5	0.0319	1.3	202.3	2.6
7	943	1976	3.4	16.7486	3.1	0.2684	4.3	0.0326	3.0	206.8	6.0
8	1316	2728	2.9	18.3857	6.8	0.2417	7.1	0.0322	1.9	204.4	3.9
9	936	6236	3.0	18.0902	5.3	0.2466	6.2	0.0324	3.2	205.3	6.4
10	826	1424	1.5	20.2006	7.5	0.2107	8.8	0.0309	4.6	196.0	8.9
11	567	14806	13.0	19.6290	1.4	0.2246	2.8	0.0320	2.5	202.9	4.9
12	1029	2182	2.2	19.1636	10.2	0.2253	10.3	0.0313	1.2	198.8	2.3
13	935	1964	0.9	19.5149	8.7	0.2223	8.9	0.0315	1.9	199.7	3.8
14	967	1194	1.0	21.1794	6.9	0.2051	7.0	0.0315	1.2	200.0	2.3
15	604	4416	3.4	17.0579	9.3	0.2620	9.3	0.0324	1.1	205.6	2.1
16	749	2640	2.3	17.5150	2.9	0.2478	4.3	0.0315	3.1	199.8	6.1
17	1125	1910	4.2	17.5672	3.0	0.2465	3.1	0.0314	0.8	199.3	1.6
18	1066	1052	1.7	19.8582	1.9	0.2218	3.0	0.0320	2.2	202.7	4.5
19	760	5796	0.9	19.0574	2.8	0.2209	5.0	0.0305	4.1	193.9	7.8
20	805	1384	0.9	22.1004	11.3	0.1945	11.7	0.0312	3.0	197.9	5.9
21	798	7760	4.4	18.7877	2.1	0.2351	3.3	0.0320	2.5	203.2	5.1

| 22 | 482 | 10430 | 2.7 | 18.7817 | 9.2 | 0.2329 | 9.8 | 0.0317 | 3.5 | 201.3 | 6.9 |
| 23 | 614 | 2670 | 1.1 | 17.7645 | 2.1 | 0.2530 | 3.3 | 0.0326 | 2.5 | 206.8 | 5.1 |

Table 4. Rb-Sr isotopic analysis of monzogranite (Fi-1) and slate

Sample	AGE (ma)	Rb (ppm)	Sr (ppm)	$^{87}Rb/^{86}Sr$	$(^{87}Sr/^{86}Sr)m$ (2σ)	$(^{87}Sr/^{86}Sr)i$ R0(Sr)
Monzogranite	201	105.5	689	0.4425	0.70804 (1)	0.706776
Slate	201	149	74.8	5.7365	0.73701 (1)	0.720613

m= measured. Errors are reported as 2σ (95% confidence limit).
R0(Sr) is the initial ratio of $^{87}Sr/^{86}Sr$ for each sample, calculated using $^{87}Rb/^{86}Sr$ and $(^{87}Sr/^{86}Sr)m$ and an age 201 (age based on zircon).

Table 5. Nd-Sm isotopic analysis of monzogranite (Fi-1) and slate

Sample	Sm ppm	Nd ppm	$^{147}Sm/^{144}Nd$	$(^{143}Nd/^{144}Nd)M$ (2σ)	$(^{143}Nd/^{144}Nd)i$ R0(Nd)	εNd I
Monzogranite	4.94	35.0	0.0853	0.512331 (07)	0.512219	-3.13
Slate	8.20	44.4	0.1116	0.511748 (07)	0.511601	-15.19

m= measured. Errors are reported as 2σ (95% confidence limit).
R0(Nd) is the initial ratio of $^{143}Nd/^{144}Nd$ for each sample, calculated using $^{147}Sm/^{144}Nd$ and $(^{143}Nd/^{144}Nd)m$ and an age of 201 (age based on zircon).εNdI, initial εNd value.

Source of magma

Initial $^{87}Sr/^{86}Sr$, εNd and $^{143}Nd/^{144}Nd$ of MORB basalts, monzogranite and slate from the study area are plotted in Figs.12-13. Initial εNd isotope values for monzogranite is -3.13 and for MORB is between +7 to +13. Initial $^{87}Sr/^{86}Sr$ isotope values for monzogranite is 0.706776 and for MORB is less than 0.704. Initial $^{143}Nd/^{144}Nd$ isotope values for monzogranite is 0.512219 and for MORB is between 0.5130 to 0.5135. Based on the isotope values monzogranite did not originated from the slate or any rock similar to slate. The isotopic values for monzogranite could be considered as representative of magma derived from lower continental crust or upper mantle which is contaminated by the crust [31 & 32].

Magnetic susceptibility of monzogranite is between 5-11 × 10^{-5} (SI units) therefore they belong to the ilmenite series of reduced type granitoids [33].   They are also moderately peraluminous.

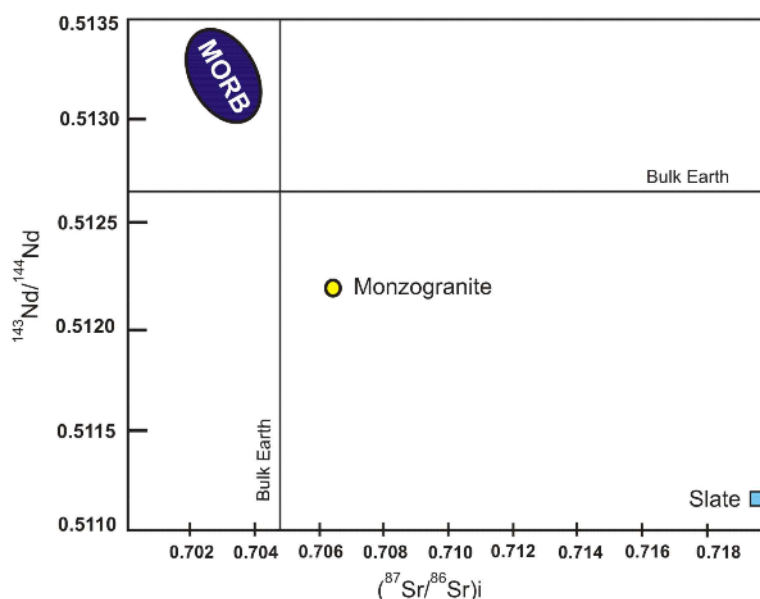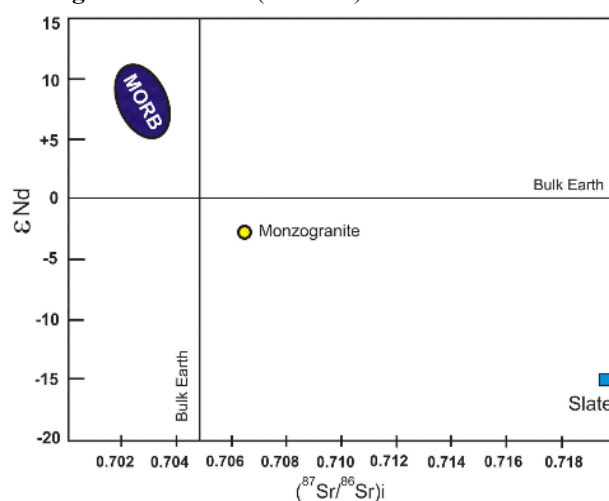**Figure 11**. Plot of $(^{87}Sr/^{86}Sr)i$ versus $^{143}Nd/^{144}Nd$.

Figure 12. Plot of $(^{87}Sr/^{86}Sr)i$ versus εnd.

Conclusions

Monzogranite is moderately peraluminous granitoid. Based on magnetic susceptibility of 5-11 $\times 10^{-5}$, the monzogranite belongs to the ilmenite series. It is characterized by strong light rare earth element (LREE) enrichment and low heavy REE (HREE) content. $(La/Yb)N$ = 32 to 56. Based on U-Th-Pb zircon age dating, monzogranite was intruded 201.3 ± 3.6 Ma, in Upper Triassic (Rhaetian) time. Based on major, trace and REE it formed during late orogenic. The initial $(^{87}Sr/^{86}Sr)i$ = 0.706776 and $(^{143}Nd/^{144}Nd)i$ = 0.512219. Initial εNd isotope value for monzogranite is -3.13. The isotopic values for monzogranite could be considered as representative of magma derived from lower continental crust or upper mantle which is contaminated in the continental crust.

Acknowledgments

References

[1] Jarchovski T., Momenzadeh M., Tadayon A., Ziegler V., *"Mineral reconnaissance in Mashhad Quadrangle"*, Geological Survey of Iran (1973) 192.

[2] Alberti A., Moazez. Z., *"Plutonic and metamorphic rocks of the Mashhad area (northeastern Iran, Khorasan)"*, Boll. Soc. Geol. Italy 93 (1974) 1157-1196.

[3] Alberti A., Nicoletti M., Petrucciani C., *"K-Ar Ages of micas of Mashhad granites"*, Period Miner. 42 (1973) 483-493.

[4] Plimer I.R., Moazez Lesco Z., *"Garnet xenocrysts in the Mashhad Granite, NE Iran"*, Geologische Rundschau. 69, 3, (1980) 801-810.

[5] Majidi B., *"The ultrabasic lava flows of Mashhad, North East Iran."*, Geological Magazine 118 1 (1981) 49-58.

[6] Alavi Mehdi, *"The Virani ophiolite complex and surrounding rocks"*, Geologische Rundschau, 68 (1979) 334-341.

[7] Alavi Mehdi, *"Sedimentary and structural characteristics of the Paleo-Tethys remnants in northeastern Iran"*, Geological Society of America Bulletin 103 8 (1991) 983-992.

[8] Alavi Mehdi, *"Thrust tectonics of the Binaloud region; NE Iran"*, Tectonics. 11 2 (1992) 360-370.

[9] Valizadeh M., Karimpour M.H., *"Origin and tectonic setting of Mashhad granitoids"*, Journal of Sciences, University of Tehran, V. 21 No. 1 (1995) 71-82.

[10] Mirnejad H., *"Geochemistry and petrography of Mashhad granites and pegmatites"*, M.Sc. thesis, Tehran University. (1991)

[11] Iranmanesh J., Sethna S.F., *"Petrography and geochemistry of the Mesozoic granite at Mashhad, Khorasan Province, northeastern part of Iran"*, Journal of the Geological Society of India. 52 1 (1998) 87-94.

[12] Abbasi H., *"Petrology of regional and contact metamorphic rocks south of Mashhad"*, M.Sc. thesis. Tehran University. (1998).

[13] Ghazi M., Hassanipak A.A., Tucker P.J., Mobasher K., *"Geochemistry and 40Ar-39Ar ages of the Mashhad Ophiolite, NE Iran"*, abstracts as: Eos. Trans. AGU, 82(47), Fall Meet. (2001).

[14] Stampfli G.M., *"The Intra-Alpine terrain: a Paleo-Tethyan remnant in the Alpine"*, Variscides. Eclogae geol. Helv. 89 (1) (1996) 13-42.

[15] Stampfli G.M., Tethyan oceans. In: E. Bozkurt, J.A. Winchester and J.D.A. Piper (Eds.), *"Tectonics and magmatism in Turkey and surrounding area"*, Geological Society of London, Special Publication 173 (2000) 163-185.

[16] Stampfli G.M., *"Opening and closure of Paleo-Tethys in Iran"*, Personal communication (2002).

[17] Stampfli G.M., Pillevuit A., *"An alternative Permo-Triassic reconstruction of the kinematics of the Tethyan realm"*, In: J. Dercourt, L.-E. Ricou and B. Vrielinck (Eds.), Atlas Tethys Palaeoenvironmental Maps. Explanatory Notes. Gauthier-Villars Paris, (1993) 55-62.

[18] Stampfli G.M., Marcoux J., Baud A., *"Tethyan margins in space and time"*, In: J.E.T. Channell, E.L. Winterer and L.F. Jansa (Eds.), Paleogeography and paleoceanography of Tethys. Palaeogeography, Palaeoclimatology, Palaeoecology 87 (1991) 373-410.

[19] Stocklin J., *"possible ancient continental margins in Iran"*, The Geology of Continental Margins, Edited by C.A. Burk & C.L. Drake, (1974) 873-887.

[20] Khatonie Molayossefi M., *"The study of stratigraphy and plants fossils of Shemshak Formation in Shandiz area"*, M.S thesis. (2000) 222.

[21] Gehrels G. E., Valencia V. A., *"Pullen in Geochronology: Emerging Opportunities"*, ed. T. Loszewski and W. Huff, Paleo. Soc. Pap., 12 (2006) 67-76.

[22] Barker F., *"Trondhjemite: definition, environment and hypotheses or origin"*, In Barker, F. (ed) Trondhjemites, dacites, and related rocks, 1-12 New York : Elsevier. (1979).

[23] Whalen J.B., Currie K.L., Chappell B.W., *"A-type granites. geochemical characteristics, discrimination and petrogenesis"*, Contributions to Mineralogy and Petrology 95 (1987) 407-419.

[24] Barbarin B., *"A review of the relationships between granitoid types, their origin and their geodynamic environments"*, Lithos 46 (1999) 605-626.

[25] Villaseca C., Barbero L., Herreros V. A. *"Re-examination of the typology of peraluminous granite types in intra continental orogenic belts"*, Transaction of the Royal Society of Edinburgh; Earth Sciences 89 (1998) 113-119.

[26] Batchelor R.A., Bowden P., *"Petrogenetic interpretation of granitoid rock series using multicationic parameters"*, Chem. Geol., 48 (1985) 45-55.

[27] Taylor S.R., McLennan S.M., *"The Continental Crust; Its composition and evolution; an examination of the geochemical record preserved in sedimentary rocks"*, Blackwell, Oxford. (1985) 312.

[28] Boynton W.V., *"Cosmochemistry of the rare earth elements; meteorite studies. In: Rare earth element geochemistry."* Henderson, P. (Editors), Elsevier Sci. Publ. Co., Amsterdam. . (1984) 63-114.

[29] Pearce J.A., Harris N.B.W., Tindle A.G. , *"Trace element discrimination diagrams for the tectonic interpretation of granitic rocks"*, Journal of Petrology 25 (4) (1984) 956-983.

[30] Majidi B., *"The geochemistry of ultrabasic and basic lava flows occurrences in northeastern Iran"*, In Geodynamic project in Iran. Geological Survey of Iran Report No. 51 (1983) 463-477.

[31] Garrido C. J., Bodinier J.-L, Burg J.-P, Zeilinger G., Hussain S., Dawood H., Chaudhry M.N., Gervilla F., *"Petrogenesis of mafic garnet granulite in the lower crust of the Kohistan Paleo-arc Complex (Northern Pakistan): Implications for intra-crustal differentiation of island arcs and generation of continental crust"*, Journal of Petrology 47 (2009) 1873–1914

[32] Zhengfu G., Wilson M., Liu J., Mao Q., *"Post-collisional, Potassic and Ultrapotassic Magmatism of the Northern Tibetan Plateau: Constraints on Characteristics of the Mantle Source"*, Geodynamic Setting and Uplift Mechanisms. Journal of Petrology Volume 47 Number 6 (2006) 1177-1220.

[33] Ishihara S., *"The magnetite-series and ilmenite-series granitic Rocks"*, Mining Geology 27 (1977) 293-305.